Proceedings of The National Conference
On Undergraduate Research (NCUR) 2020
Montana State University, Bozeman MT
March 26-28, 2020

Rapid Filtration Through Nanosculpted Silicon Membranes

Nathaniel Michek, Angelica Drees, David Rohr, and Nathan Shannon
Engineering Physics
University of Wisconsin-Platteville
1 University Plaza
Platteville, WI 53818

Faculty Advisor: Dr. Gokul Gopalakrishnan

Abstract

The separation of microscopic particles and biological entities such as proteins, viruses, and bacteria, is often carried out using membrane filtration. This process uses a filter, typically made from a flexible polymer membrane several micrometers thick, with cylindrical or prismatic pores having parallel sidewalls. At the micro and nano-scales, filtration through these traditional membrane systems can take significant time due to the high flow resistance arising from the membrane thickness and the geometry of the pore sidewalls. Modeling flow rates through different types of pore geometries using computational fluid dynamics techniques, we find large increases in the speed of filtration by replacing pores having parallel walls with pores having angled sidewalls. We have developed a process to fabricate membranes with significantly reduced thickness, possessing pores with suitably tapered sidewalls. These silicon nanomembranes are thin suspended sheets of single crystal silicon, with high strengths despite having thicknesses lower than a micrometer. We use a focused electron beam and selective, anisotropic etch processes to create nanoscale openings in the membranes that possess pyramidal sidewalls for reduced flow impedance. This paper focuses on fluid dynamics simulations of these micro and nano-scaled pore structures in silicon nanomembranes.

Keywords: Nanomembranes, Filtration, Microfluidics, Molecular Sieves

1. Introduction

The separation of particles and macromolecules from liquids is carried out in a variety of fields, from biomedical diagnostics and drug discovery to water sampling and purification. These separations are carried out through one of several techniques such as chromatography[1], mass spectroscopy[2], electrophoresis[3], inertial focusing[4], and membrane-based molecular weight cutoff filtration[5]. Membrane filtration is commonly used due to its low cost, relatively high selectivity, and ease of setup. Precision membrane filters several micrometers thick with parallel-walled prismatic pores can take significant time to filter even small volumes of fluid due to the high flow impedance arising from the sidewall geometry. Advances in semiconductor nanofabrication have yielded the ability to fabricate thin, nanoscale membranes from silicon, that can be etched to create porous filters[6,7]. More recently, nanomembranes have been fabricated from single-crystal silicon that possess mechanical properties comparable to much thicker polymeric membranes[8]. Furthermore, these single-crystalline nanomembranes can be anisotropically etched to create micro- to nanoscale pores with pyramidal sidewalls. We explore the potential flow rate benefits of replacing prismatic pores in traditional microscale polymeric membranes with pyramidal pores in single-crystal silicon nanomembranes.

2. Methods

2.1. Fabrication of Porous Nanomembranes

A silicon membrane is a thin, flat, suspended sheet of crystalline silicon fabricated by photolithography and etching, from a larger single crystal wafer of silicon-on-insulator (SOI)[8]. These nanomembranes are often tens to hundreds of nanometers thick and are formed from the silicon device layer of the parent SOI wafer, as described in Ref. 8, and shown in Fig. 1(i) here. Additional process steps, described in detail in a separate manuscript, including photolithographic patterning and selective etching are used to first create a membrane structure, as depicted in Fig. 1(ii). Subsequently, electron beam lithography and anisotropic etching are used to create pyramidal pores (see Fig. 1(iii)) that are micrometers to nanometers in opening size. Fig. 1(iv) is a scanning electron microscope image showing 400 nm wide pore openings at the bottom of a 100 nm thick silicon nanomembrane, created using this process.

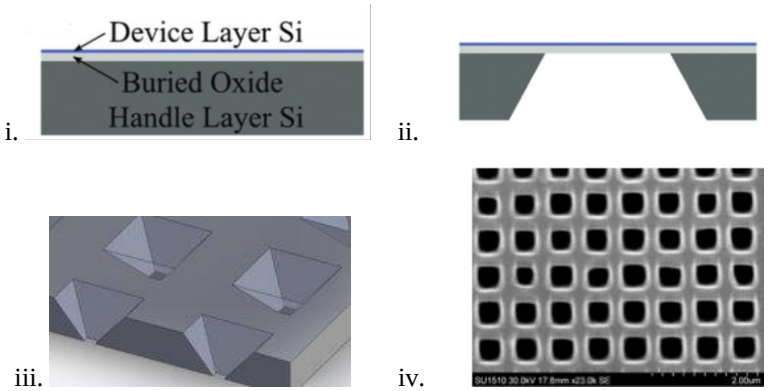

Figure 1. Nanopatterned openings in 100 nm thick silicon membranes

2.2. Fluid Flow Modeling

The flow rates of pure water through three different pore geometries were estimated using analytical approximations and computational fluid dynamics (CFD) simulations. The pores we examined include: (i) prismatic pores in thick membranes, with pore length (i.e.: membrane thickness) much larger than the pore width, (ii) prismatic pores in thin membranes with pore lengths comparable to pore widths, and (iii) pyramidal pores in thin membranes, where the pore length is comparable to the size of the opening on the narrower end of the pyramidal pores. In all subsequent descriptions, we refer to these pores respectively as (i) deep prismatic pores, (ii) shallow prismatic pores, and (iii) shallow pyramidal pores. A comparison of the pore geometries is shown in Fig. 2.

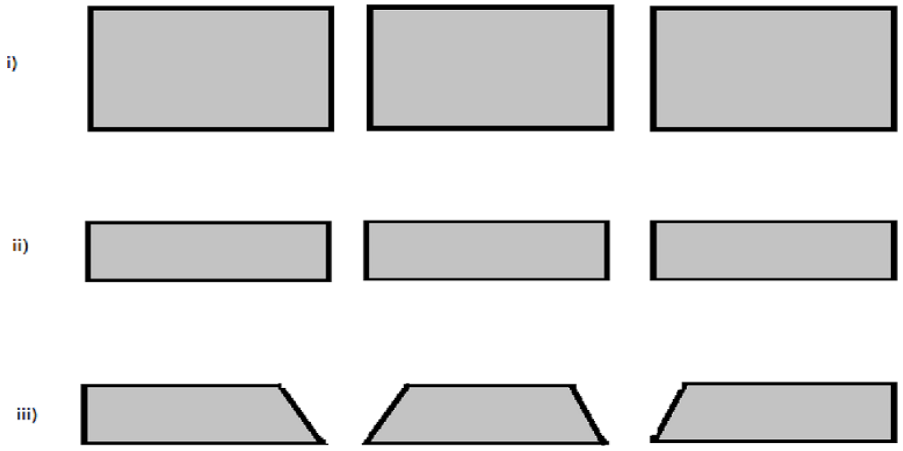

Figure 2. Membranes with (i) deep prismatic pores, (ii) shallow prismatic pores, and (iii) shallow pyramidal pores.

The Hagen-Poiseuille's law was used on each of the pore geometries. Equation 1 shows the generalized form of the Hagen-Poiseuille's law that describes the volumetric flow rate, *Q*, for prismatic pore configurations with circular cross sections[9].

$$Q = \frac{\Delta P \pi r^4}{8 \mu l} \tag{1}$$

Here, ΔP represents the pressure difference across the membrane, r is the pore radius, , μ is the viscosity, and l is the length of the pores, which, in all of the cases examined, is equal to the thickness of the membrane. When using pore openings other than circles the radius can be determined by the hydraulic diameter. Equation 2 shows a modified form of the Hagen-Poiseuille's law applicable for conical pores, derived by considering the variation in the pore width due to angled sidewalls. We use this to approximate the flow rate through pyramidal pores[10].

$$Q = \frac{\Delta P}{\int_0^l \frac{\mu\left(3+\frac{8}{\pi}\right)}{r^3(z)} \frac{dz}{r(z)}} \tag{2}$$

$$r(z) = r_o + z \tan\theta, \tag{3}$$

where $r(z)$ is the changing radius of the pore as a function of height, z, measured from the membrane bottom surface where the radius is r_o, and θ is the sidewall angle measured from the membrane normal, and is typically about 35° for single crystal silicon membranes.

The CFD simulations were performed using STAR CCM+ under steady state conditions with laminar flow and the no slip boundary condition. Additionally, a segregated finite volume solver was used, and mesh analysis was performed. All simulations have been performed under the assumption that flow through a single pore is independent of the flow through neighboring pores in the membrane. In order to make a comparison, all tests in both the analytical and CFD models were run with pore openings between 100 nm and 500 nm, and a pressure differential of 1 atm to best replicate experimental conditions commonly encountered in the use of these membrane filters.

3. Results

Both the analytical and CFD simulations results show a significant decrease in the resistance to flow for the pyramidal pores as compared to the prismatic pores. When looking at the CFD results for each of the pore geometries the Poiseuille flow velocity profile is observed, as seen in Fig. 3.

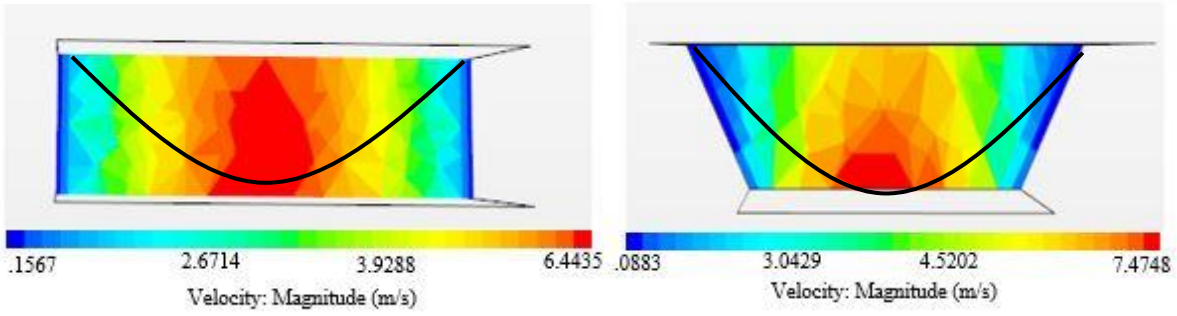

Figure 3. Scalar velocity plots and generalized Poiseuille flow profiles for (i) shallow prismatic pores, (ii) shallow pyramidal pores, both with 300 nm bottom opening sizes the average flow velocity for the prismatic pores is 2.97 m/s, while the pyramidal pores average flow velocity is 4.38 m/s.

Fig. 4 compares analytical and numerical models of each of the set ups in terms of velocity. Shallow pores offer significantly reduced flow impedances compared to deep pores in proportion to the pore length and can easily reach an order or two of magnitude reduction. When compared with prismatic pores, pyramidal pores offer a further reduction of impedance up to an order of magnitude when pores are below 100 nm across. These reductions become significant when comparing the deep prismatic pores present in traditional polymeric membranes, with the shallow pyramidal pores possible with single crystalline nanomembranes.

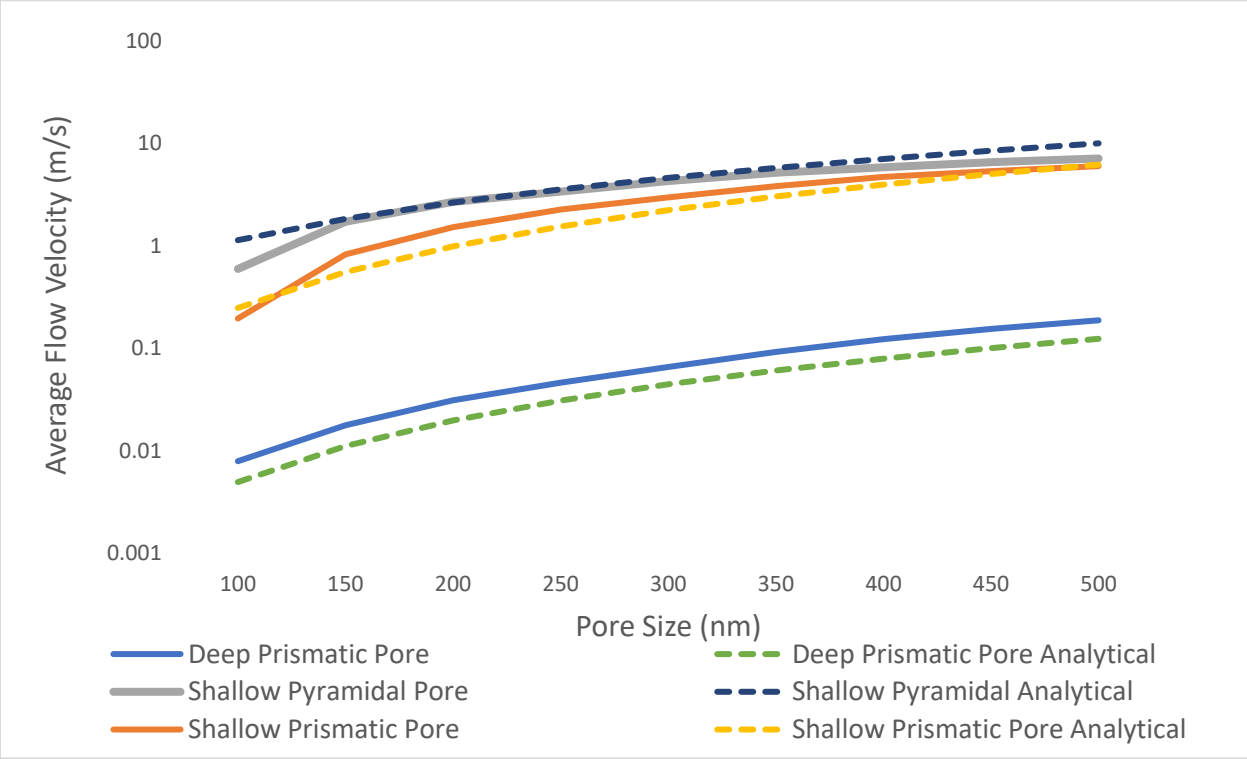

Figure 4. Comparison of analytical and numerical results for each pore shape.

The improvement in flow rate through pyramidal pores becomes most noticeable at pore opening sizes comparable or smaller than the membrane thickness, making this style of membrane filter particularly valuable in the trapping and detection of sub-micron objects such as viruses.

4. Conclusions

As shown by both the analytical and CFD results, shallow pyramidal pore structures can decrease the amount of time needed to carry out filtrations in the micro to nano-scale regimes, by orders of magnitude compared to prismatic pores in traditional polymeric membranes. Due to this significant decrease in flow impedance, several membranes with varying pore sizes can be stacked in series to simultaneously separate species of different sizes in a single filtration cycle. These characteristics make nanomembrane filters promising candidates for use in detecting waterborne pathogens like viruses and bacteria[11,12] or disease-causing prions in livestock and wildlife[13].

5. Acknowledgements

The authors wish to express their appreciation to Dr. Gokul Gopalakrishnan, Dr. Lee Farina, Dr. Mark Levenstein and Dr. Jorge Camacho for their mentorship and advice. We acknowledge funding from the University of Wisconsin System through the Regent Scholar and Dairy Innovation Hub programs.

6. References

1. E. Ruckenstein and D.C Prieve, "Adsorption and desorption of particles and their chromatographic separation," AIChE 22 (1976):276.

2. Pawel L. Urban, "Quantitative mass spectrometry: an overview," Philos Trans A Math Phys Eng Sci 374 (2016), https://www.ncbi.nlm.nih.gov/pmc/articles/PMC5031646/.

3. Timothy Ter Ming Tan and all, "Gel eletrophoresis," Biochemistry and Microbiology Education 35 (2007), https://iubmb.onlinelibrary.wiley.com/doi/10.1002/bmb.83 .

4. M. Masaeli, and others, "Continuous Inertial Focusing and Separation of Particles by Shape," Physical Review X 2(2012).

5. Rosiah Rohani, and others, "A refined one-filtration method for aqueous based nanofiltration and ultrafiltration membrane molecular weight cut-off determination using polyethylene glycols," Journal of Membrane Science, 382:1-2, (2011): 278, https://purehost.bath.ac.uk/ws/portalfiles/portal/227698/Patterson_JMS_2011_382_1-2_278.pdf

6. Albert van den Berg and Matthias Wessling, "Silicon for the perfect membrane," *Nature 445* (2007).

7. C. C. Striemer, and others, "Charge- and size-based separation of macromolecules using ultrathin silicon membranes," *Nature 445*,(2007): 749.

8. G. Gopalakrishnan, and others, "Edge-induced flattening in the fabrication of ultrathin freestanding crystalline silicon sheets," Applied Physics Letters 102 (2013).

9. A. Plecis, and others, "Flow Control in Microfluidic Devices," Elveflow, www.elveflow.com.

10. John A. Rogers and Jong-Hyun Ahn, Silicon Nanomembranes: Fundamental Science and Applications, (Weinheim: Wiley-VCH Verlag GmbH & Co., 2016), 244.

11. World Health Organization, "Results of Round I of the WHO International Scheme to Evaluate Household Water Treatment Technologies," *Water Sanitation and Health* (2016).

12. Gabriel Bitton, Microbiology of Drinking Water Production and Distribution, (Hoboken: John Wiley and Sons, 2014), 312.

13. T. R. John, and others, "Early Detection of Chronic Wasting Disease Prions in Urine of Pre-symptomatic Deer by Real Time Quaking Induced Conversion Assays," Prion, 7:3 (2013): 253, https://www.tandfonline.com/doi/pdf/10.4161/pri.24430?needAccess=true .